Signal-dependent reactivity of host-guest complexes controls supramolecular aggregate formation

Li, Guotai; Wan, Yucheng; Lewis, Reece W.; Fan, Bowen; Eelkema, Rienk

Important note
To cite this publication, please use the final published version (if applicable).
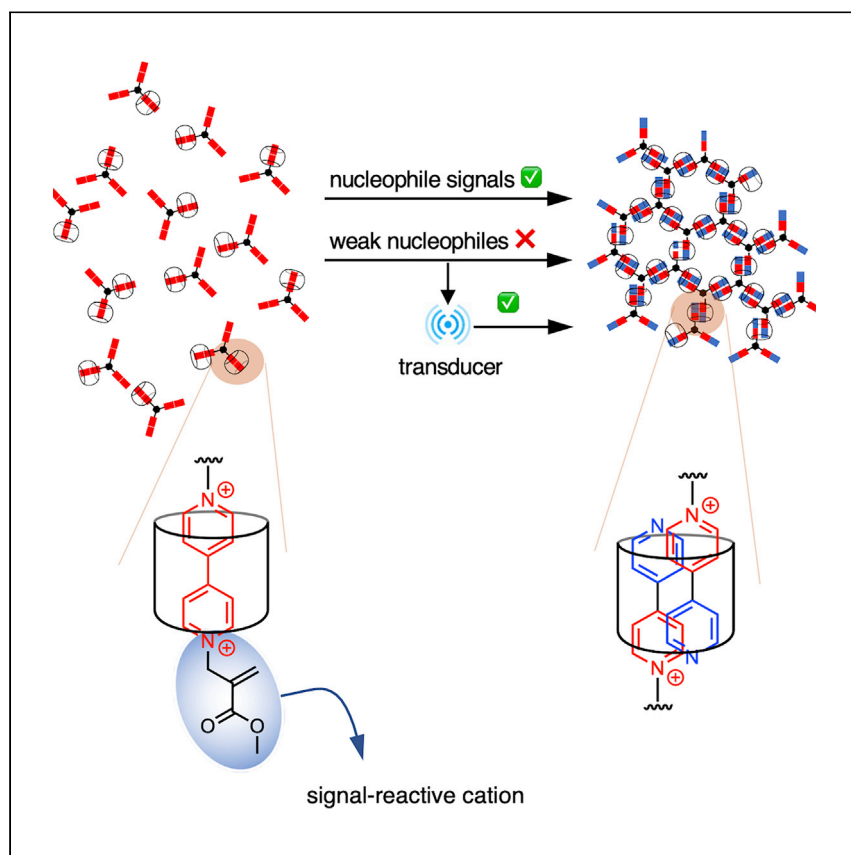Please check the document version above.

Article

Signal-dependent reactivity of host-guest complexes controls supramolecular aggregate formation

Li et al. report control over supramolecular aggregation based on host-guest interaction using a range of biological signals where the aggregation rate highly depends on signal reactivity. They expand this concept to other signals by developing a signal relay strategy, demonstrated by showing response to weakly nucleophilic hydrogen peroxide.

Guotai Li, Yucheng Wan, Reece W. Lewis, Bowen Fan, Rienk Eelkema

r.eelkema@tudelft.nl

Highlights

A range of nucleophilic signals are applied to trigger host-guest aggregation

Aggregation rates are closely related to signal reactivity

Signal nucleophilicity controls aggregate morphology and crystallinity

Signal relay enables effective response to weakly nucleophilic H_2O_2

Article

Signal-dependent reactivity of host-guest complexes controls supramolecular aggregate formation

Guotai Li,[1] Yucheng Wan,[1] Reece W. Lewis,[1] Bowen Fan,[1] and Rienk Eelkema[1,2,3,*]

SUMMARY

Living systems can respond to their environment through signal transduction cascades. In these cascades, original stimuli are amplified and translated into reaction or assembly events. In an effort to instill synthetic materials with biomimetic responsivity, we report an aggregation process forming a supramolecular network held together by host-guest interactions that is responsive to nucleophilic chemical signals through a chemical reaction-assembly cascade. In particular, we developed a signal-induced switch between cucurbit[8]uril binary and ternary complexes with cationic bipyridine derivatives where the charge on the bipyridine can be changed through an allylic substitution reaction with the nucleophilic signal. When applied to a multitopic bipyridine guest, the reaction with the nucleophile signals leads to supramolecular network formation where the aggregation rates and final structure depend on the nucleophilicity of the signal. This work opens the door to new opportunities for signal-responsive synthetic materials and interactions with biological systems.

INTRODUCTION

Processing specific signals leading to triggering of event cascades is a hallmark of living systems. An example of such a cascade is platelet aggregation and fibrin formation leading to blood coagulation, activated by agonists after vascular trauma.[1] Importantly, such a cellular response is typically realized not by directly reacting to the primary stimulus but by multiplexed signal transduction cascades transduced by receptors and switchable enzymes, causing the cell to respond to the initial stimulus.[2] In efforts to instill artificial materials with biomimetic responsivity, supramolecular materials have attracted much attention over the last two decades owing to the dynamic and reversible nature of non-covalent bonding.[3,4] These materials can have the ability to adapt to environmental stimuli,[3] including physical cues (temperature,[5,6] light[7–10]) or chemical signals (pH,[11–13] ions,[14] redox agents,[15,16] and non-covalent interactions[17]). However, supramolecular assemblies that are responsive to biologically relevant small molecules via chemical reaction cascades remain limited.[18]

Host-guest complexation is one of the most widely explored non-covalent interactions in the area of supramolecular materials.[19,20] A well-known host-guest pair is the viologen moiety[21] with cucurbit[8]uril (CB[8]). Viologen forms a stable, high-association-constant, 1:1 complex with CB[8] in aqueous media through the ion-dipole interactions of dipyridinium with the CB carbonyl rims. This complex converts to a 1:2 homoternary complex upon either direct reduction (by, e.g., sodium dithionite[22])

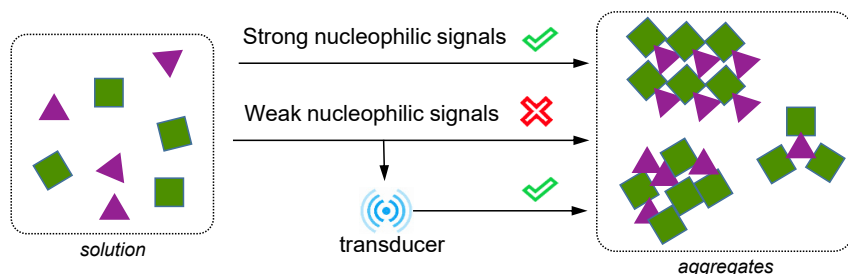[1]Department of Chemical Engineering, Delft University of Technology, Van der Maasweg 9, 2629 HZ Delft, the Netherlands

[2]Twitter: @eelkemalab

[3]Lead contact

*Correspondence: r.eelkema@tudelft.nl

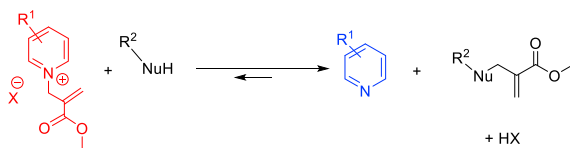https://doi.org/10.1016/j.xcrp.2023.101309

A   Signal induced aggregate formation and signal transduction

B   Substitution reaction with β'-pyridinium acrylic ester Michael acceptor

R²NuH: Biological nucleophiles (thiols, amines, alcohols)

Scheme 1. Control of supramolecular systems through chemical signaling
Signal induced aggregate formation strategy (A), and substitution reaction of nucleophiles with Michael acceptors with an allylic quaternary ammonium leaving group (B).

or photoreduction[10] of viologen from the dicationic form to the radical monocation.[23,24] The reverse process can take place through chemical[25] or electrochemical[26] oxidation. Incorporation of this reversible switch in a supramolecular material makes the material responsive to redox[27,28] or photochemical stimuli.[10,25,28,29] Moreover, a similar conversion between binary and homoternary complexes can also be achieved through protonation/deprotonation of bipyridine.[12,13,30,31] Nevertheless, reports of host-guest complexes that are responsive to biological signals through chemical reaction cascades remain rare.

Our work builds on a recently reported reversible allylic substitution of Michael acceptors[32] that has also been applied to design chemoresponsive materials such as polymer hydrogels[33] and block copolymer complex coacervate core micelles.[34] When these Michael acceptors have an allylic quaternary ammonium leaving group, the reaction of a nucleophile with the Michael acceptor leads to elimination of a tertiary amine and the removal of positive charge (Scheme 1B). Crucially, cationic functionalities on a guest molecule can contribute strongly to their binding affinity with CB[8].[35] Combining these concepts, we hypothesize that binding of guests to CB[8] can be controlled using the nucleophile-triggered allylic substitution. Relevant nucleophilic species such as amines and thiols are abundant in biological systems (e.g., amino acids, dopamine, glutathione [GSH]) and also in many drugs. Developing host-guest interactions responsive to biological signals constitutes a route to endow artificial materials with biomimetic functionality.

In this work, multiple biological nucleophilic species are applied as signals to control aggregation processes based on host-guest complexation. In addition, mimicking biochemical signaling cascades, a signal transducer is introduced, by which unreactive or weakly reactive signals can be applied as an effective trigger of aggregation (Scheme 1A). This signal transduction strategy can further broaden the range of possible signals.
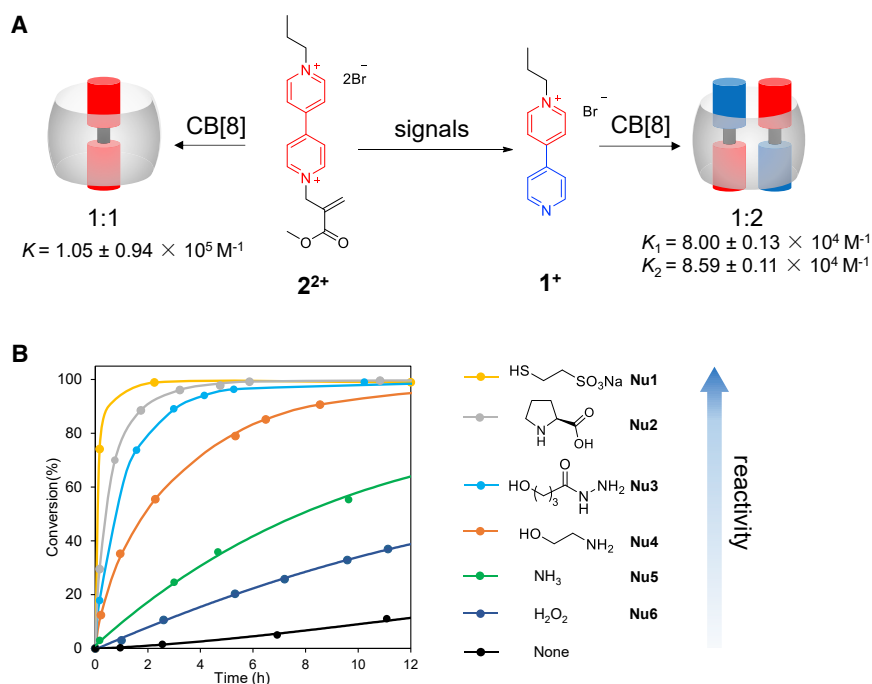
A

B

Figure 1. Nucleophilic signals induced charge removal and differential binding of bipyridinium derivatives to CB[8]

(A) Structures of bipyridinium derivatives used in this work and their binding affinity to CB[8] (determined by ITC, 50 mM sodium phosphate buffer [pH 7.4]).

(B) Conversion of 2^{2+} upon reaction with different nucleophilic signals followed by ^{1}H-NMR (50 mM sodium phosphate buffer with 10% D_2O), $[2^{2+}]$ = 2 mM, [signals] = 3 mM.

RESULTS AND DISCUSSION

Reactivity of nucleophilic species and host-guest binding properties

We first studied the host-guest binding properties of CB[8] with bipyridine derivatives. Monocationic pyridinium (1^{1+}) was synthesized by alkylating 4,4′-bipyridine with propyl bromide at one nitrogen. Further reaction with methyl 2-(bromomethyl)acrylate results in dicationic guest molecule 2^{2+} with one permanent and one removable cation. Nuclear magnetic resonance (NMR) titration and isothermal titration calorimetry (ITC) showed that these two guest molecules bind with CB[8] in 2:1 and 1:1 ratios, respectively, which is in line with reported results.[30] In 50 mM sodium phosphate buffer solution, the binding constant of 1^{1+} with CB[8] was determined by ITC as $K_1 = 8.00 \times 10^4$ M^{-1}, $K_2 = 8.59 \times 10^4$ M^{-1}, 2^{2+} with CB[8] as $K = 1.05 \times 10^5$ M^{-1} (Figure 1A).

We then tested the reactivity of different nucleophiles as chemical signals to remove a charge from the dicationic guest molecule 2^{2+}. Considering differences in structure and reactivity, we selected a thiol (Mesna,[36] **Nu1**, a drug); a secondary amine (L-proline, **Nu2**, an amino acid); a hydrazide derivative (**Nu3**, hydrazides are metabolic intermediates[37]); primary amine (ethanolamine, **Nu4**, abundant in biological membranes); NH$_3$ (**Nu5**, metabolic waste); and H$_2$O$_2$ (**Nu6**, cellular reactive oxygen species) as representative nucleophiles. It should be noted that some hydrazide derivatives form as intermediates in metabolic processes, but we do not apply these specific hydrazides in this work. Instead, we use 4-hydroxybutanohydrazide (**Nu3**), which is water soluble and has low affinity for cucurbiturils.[38]

Figure 2. Signal-induced aggregation of a tricationic guest with CB[8]

(A) Schematic overview of the signal-induced aggregation process; Br⁻ counterions are omitted.

(B) Representative photographs of turbidity changes of samples ([4^{6+}] = 0.3 mM, [CB[8]] = 0.45 mM) without signals (left) and 24 h after adding proline (right, **Nu2**, 0.9 mM).

(C) Turbidity measurement (transmittance at 500 nm, [4^{6+}] = 0.3 mM, [CB[8]] = 0.45 mM, [signals] = 0.9 mM).

(D and E) DLS measurements, [4^{6+}] = 0.1 mM, [CB[8]] = 0.15 mM, [signals] = 0.3 mM in 50 mM sodium phosphate buffer (pH 7.4). The inset in (D) shows how the scattering count rate changes between t = 0.9 and 1.4 h.

Using ^{1}H-NMR spectroscopy, we followed the conversion of 2^{2+} (2 mM) upon reaction with 3 mM signal molecules (in 50 mM sodium phosphate buffer [pH 7.4]). For Mesna, L-proline, and ethanolamine, the reaction rates agree very well with the reported nucleophilicity[39] as thiol > sec. amine > prim. amine (Figure 1B). Where Mesna gave >90% conversion in a 1 h reaction, proline reached ∼70% and ethanolamine 35% in the same time. Interestingly, 4-hydroxybutanohydrazide has a reactivity comparable to proline, reacting much faster than ethanolamine. Aqueous ammonia and hydrogen peroxide (generally considered as weak nucleophilic species) can also react with 2^{2+}, with aqueous ammonia reacting faster than hydrogen peroxide. Both nucleophiles react faster than the non-zero background reaction.

Host-guest aggregation controlled by nucleophilic signals

After exploring the CB[8] binding properties of these bipyridine derivates and their reactivity to small-molecule chemical signals, we hoped to control the formation of larger supramolecular materials. 2D and 3D supramolecular organic frameworks (SOFs) based on cucurbituril were recently developed,[40–44] showing promising application in drug[43] and DNA[44] delivery. For SOFs formed by CB[8]-dimerization of hydrophobic aromatic segments, 4-aryl-pyridinium units are the earliest and also most frequently reported binding motifs in multitopic guest molecules.[45]

As discussed above, the monocationic pyridinium (1^{1+}) can be generated by reaction of 2^{2+} with various signals, leading to the formation of the 2:1 complex with CB[8]. Based on this knowledge, we expected that a star-shaped tripodal guest with Michael-acceptor-activated dicationic arms would form discrete monomeric complexes with CB[8]. Conversion of the dicationic arms to monocations, triggered by a reaction with the nucleophile signals, would then initiate the formation of a non-covalent network by cross-linking with CB[8] (Figure 2A).

To test this hypothesis, we synthesized the tricationic guest 3^{3+} by alkylating 4,4′-bipyridine with 2,4,6-tribromomesitylene (supplemental experimental procedures 1.2). Further alkylation with methyl 2-(bromomethyl)acrylate gives the 4^{6+} guest, having 3 pyridinium arms and 6 charges. With these two multicationic guest molecules in hand, we first tested their complexation with CB[8]. 3^{3+} (0.1 mM) and CB[8] (0.15 mM) in 50 mM phosphate sodium buffer (pH 7.4) remain a heterogeneous mixture after sonicating and heating at 40°C for more than 0.5 h. After filtration with a 200 nm syringe filter at room temperature, this sample was analyzed using dynamic light scattering (DLS). Starting from a clear solution, the light scattering intensity gradually increased to 1.4 Mcps (Figure S19A), with particle diameters growing to 3.5 μm over the course of 20 h (Figure S19B). In contrast, a solution of 4^{6+} and CB[8] under the same conditions remains transparent for over 24 h, confirming that 3^{3+} and CB[8] will form a network but 4^{6+} and CB[8] will not. We then wanted to control this aggregation process using the signal molecules described above. As an initial estimate of aggregation, we quantified the turbidity by measuring the transmittance at 500 nm of samples made by mixing 4^{6+} (0.3 mM) and CB[8] (0.45 mM) in phosphate buffer (50 mM, pH 7.4). The 4^{6+}/CB[8] samples are transparent, but shortly after the addition of nucleophilic signals, the transmittance starts to decrease sharply (Figures 2B and 2C). Notably, the addition of Mesna leads to a rapid increase of turbidity (transmittance goes from 100% to <5%) within 10 min (Figure 2C). To figure out what effect is at the root of this dramatic change, we further tested sodium vinylsulfonate and 2-mercaptoethanol (Nu7) as signals. While we observed no variation of turbidity after adding sodium vinylsulfonate to 4^{6+}/CB[8] (Figure S14A; monitored for 10 h), the addition of 2-mercaptoethanol (Nu7) leads to a very similar change in turbidity as observed for Mesna. This indicates that the thiol-mediated

removal of the Michael acceptor indeed controls aggregation, while there are only limited effects of the electrostatic interactions of the sodium salt with the multicationic guest molecule. For both L-proline (**Nu2**) and hydrazide (**Nu3**) as signals, aggregation did not occur until much later (1.5 h after addition), which is in agreement with their reactivity in the small-molecule study. The relation between signal nucleophilicity and aggregation timescale was further confirmed when using ethanolamine (**Nu4**) and NH_3 (**Nu5**), leading to aggregation timescales of 3 and 7 h, respectively. When adding either H_2O_2 (**Nu6**) or no signal, no aggregation is observed during the measurement time (>10 h). We then further investigated the aggregation of 4^{6+} (0.1 mM) and CB[8] (0.15 mM) using DLS. DLS shows that, in agreement with the turbidity test, aggregation immediately starts upon adding thiol signals (Mesna [**Nu1**] and 2-mercaptoethanol [**Nu7**]), with scattering counts increasing to 22 and 18 Mcps, respectively, and particle sizes increasing to 2.5 μm (Figure S20B). The larger scatter count observed with Mesna may be caused by an additional salt effect. Addition of L-proline (**Nu2**) and hydrazide (**Nu3**) give very similar aggregation profiles, both starting ∼5 h after addition and continually increasing to 6 Mcps. With ethanolamine (**Nu4**), aggregation is observed after 14 h. The addition of NH_3 (**Nu5**) or H_2O_2 (**Nu6**) caused much smaller increases in scatter count compared with the stronger nucleophiles, barely higher than the background scattering rate.

Characterization of host-guest aggregates

Cryoelectron microscopy (Cryo-EM) images show that the aggregates made with either 2-mercaptoethanol (**Nu7**) or L-proline (**Nu2**) as signals are made up from much smaller structures. The aggregate formed using **Nu7** shows periodic structures of ∼1.8 nm in width (Figure 3A). In contrast, aggregates formed by a reaction with **Nu2** are spheroids with diameters of 9.40 ± 1.51 nm (Figure 3B). These small aggregates may subsequently assemble into larger structures (as observed in the turbid reaction mixtures), but these were not observed in cryo-EM. Avrami analysis[46–49] (Figure S21) shows a significant difference in the Avrami coefficient n between these two samples, with n = 2.81 (**Nu7**) and n = 1.85 (**Nu2**), which indicates a higher dimensionality of the growth process in the sample triggered by 2-mercaptoethanol. This result is in line with the higher dimensionality observed in the cryo-EM images. In previously studied supramolecular gelation processes, we observed increased fiber branching at higher rates of gelator formation.[46] Analogously, the current results suggest that stronger nucleophiles lead to faster complex formation and, with that, more branching. Powder X-ray diffraction (XRD) shows that both samples exhibit some crystallinity (Figure S22),[50] while the aggregate induced by 2-mercaptoethanol shows more crystalline characteristics than that from L-proline. The XRD profile of the aggregates formed by reaction with **Nu7** exhibits peaks at 17.7, 8.80, and 5.85 Å, matching very well with the periodicity of 1.8 nm observed in cryo-EM. Results from cryo-EM and XRD suggest that the morphology and crystallinity of the aggregate formed in this system can be controlled by signals with different nucleophilicity. Continuous monitoring of the aggregation process (4^{6+} [0.3 mM], CB[8] [0.45 mM], **Nu7** [0.9 mM]) by confocal laser scanning microscopy (CLSM) shows that in the beginning, the aggregates are very small, fast moving particles, which over time grow and connect together to become a larger aggregate (Video S1; Figure S15). We analyzed the composition of these aggregates over the course of the process using ^{1}H-NMR spectroscopy (supplemental experimental procedures 1.9, Figures S13 and S14, and Scheme S1). A transparent solution of 4^{6+} (0.8 mM) and CB[8] (1.2 mM) in 50 mM phosphate buffer (pH 7.4, 10% D_2O) shows the ^{1}H-NMR peaks of the $4^{6+} \subset$ CB[8] complex and of CB[8] itself. The addition of 2-mercaptoethanol results in immediate precipitation in the NMR tube, which leads to the complete disappearance of the peaks of 4^{6+} and CB[8], indicating that they
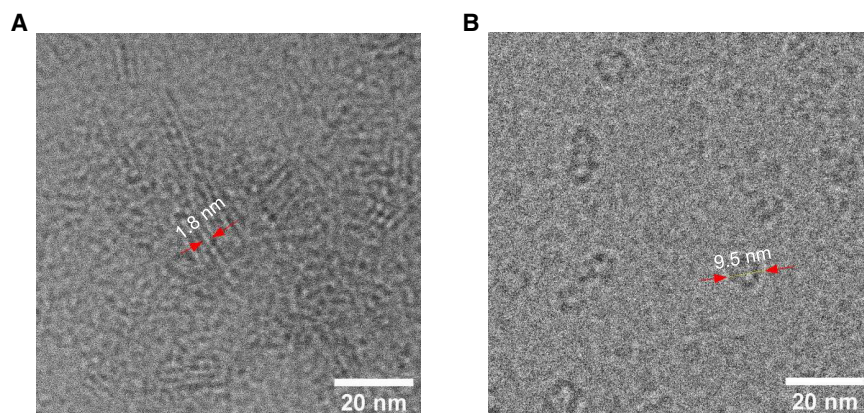
Figure 3. Cryo-EM measurement of aggregates formed using thiol and amine signals ([4^{6+}] = 0.1 mM, [CB[8]] = 0.15 mM)

(A) Image taken 24 h after adding 2-mercaptoethanol (**Nu7**, 0.3 mM), scale bar: 20 nm.

(B) Image taken 3 days after adding L-proline (**Nu2**, 0.3 mM), the average diameter is (9.40 $\pm$ 1.51) nm; scale bar: 20 nm.

are no longer in solution (Figure S17). The isolated precipitates were found to be insoluble in D_2O. We selected N,N,N-trimethyl-1-adamantylammonium chloride[51] as a soluble guest molecule with very high affinity for CB[8]. This high-affinity guest is expected to break the cross-links in the aggregate by replacing 3^{3+} in the CB[8] cavity. After mixing N,N,N-trimethyl-1-adamantylammonium chloride (24 mM) with the 3^{3+}/CB[8] precipitate in D_2O, we observed that part of the precipitate dissolved, and ^{1}H-NMR peaks of unbound 3^{3+} and CB[8] emerged (Figure S18). In this way, we demonstrate that the aggregates are indeed held together by 3^{3+}/CB[8] cross-links.

Signal transducer to trigger aggregation

These results demonstrate that aggregation can be triggered by various signals and that the aggregation rate scales with the signal nucleophilicity. However, the weak nucleophile hydrogen peroxide (**Nu6**) did not function as a signal in this cascade. H_2O_2 is generated in numerous biological systems and plays an important role in cellular processes,[52] including the role of signaling molecule to regulate a wide variety of biological responses[53] and indicating the development of various diseases.[54] In an attempt to adapt hydrogen peroxide as a signal in our signaling cascade and inspired by our previous work on H_2O_2-activited organocatalysts[55,56] we designed a relayed transduction system to amend the nucleophilicity of H_2O_2. We used a blocked proline nucleophile, protected with a boronic acid-responsive self-immolative group that can be oxidatively cleaved by hydrogen peroxide. This pre-proline functions as a signal relay (Figure 4A) where proline released by H_2O_2 will trigger aggregation. Based on this design, we first tested the reactivity on small molecules. Pre-proline (**5**) is stable in the buffer solution, but adding H_2O_2 (3 mM, 1 equiv) leads to >95% release of proline within 30 min (Figure 4B). Moreover, pre-proline shows no significant reactivity with 2^{2+}, with a 2^{2+} conversion rate close to the background reaction (Figure 4C). As discussed above, the reactivity of H_2O_2 to 2^{2+} is low (Figure 1B), but in the solution of 2^{2+} (2 mM) and pre-proline (3 mM), a high conversion rate of 2^{2+} was observed upon adding H_2O_2. Meanwhile pre-proline **5** itself shows no affinity with CB[8], as indicated by ITC (Table S1). We subsequently moved on to applying this signaling cascade to the signal-induced aggregation process. In the turbidimetry assay, H_2O_2 or pre-proline alone added into the solution of
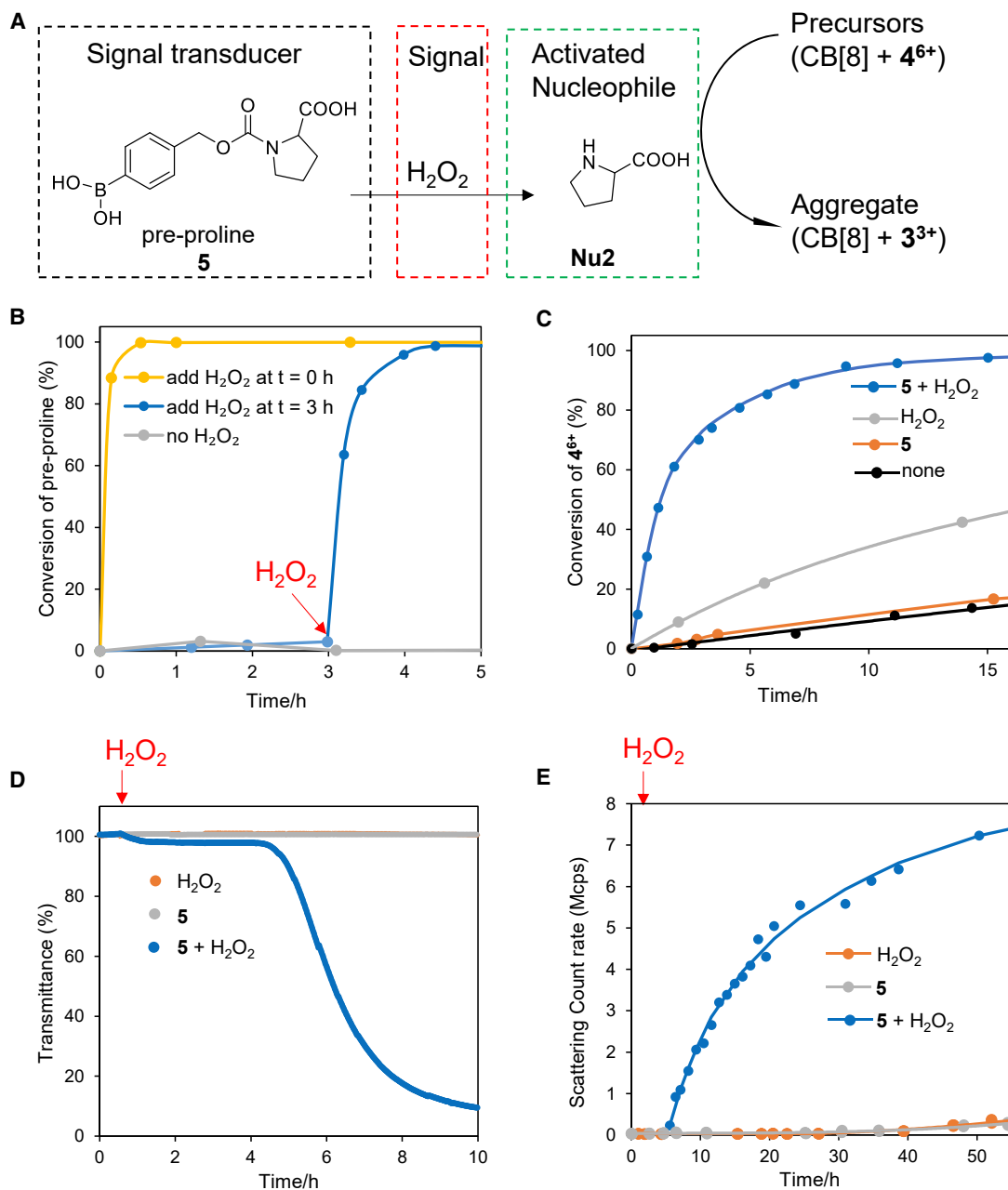
Figure 4. Pre-proline as a signal transducer to relay hydrogen peroxide to a nucleophilic signal

(A) Schematic description of the design.

(B) Conversion of pre-proline ([**5**] = 3 mM, H_2O_2 = 3 mM).

(C) Conversion of 2^{2+} through signaling cascade by H_2O_2 ([2^{2+}] = 2 mM, [**5**] = 3 mM, [H_2O_2] = 3 mM).

(D) Turbidity measurement by UV-visible (UV-vis) transmittance at 500 nm, [4^{6+}] = 0.3 mM, [CB[8]] = 0.45 mM, [**5**] = 0.9 mM, [H_2O_2] = 0.9 mM.

(E) DLS measurement of aggregate formation, [4^{6+}] = 0.1 mM, [CB[8]] = 0.15 mM, [**5**] = 0.3 mM, [H_2O_2] = 0.3 mM in 50 mM sodium phosphate buffer (pH 7.4).

4^{6+} (0.3 mM) and CB[8] (0.45 mM) did not cause any changes of transmittance. Instead, H_2O_2 (0.9 mM) added to a solution of pre-proline (0.9 mM), 4^{6+} (0.3 mM), and CB[8] (0.45 mM) instantly caused a slight decrease in transmittance, with a sharp decrease observed after ~5 h. The slower aggregation observed in this signaling cascade compared with using proline itself as a signal can be attributed to the

time it takes to release proline by H_2O_2. In the DLS measurement, at a lower concentration of 4^{6+} (0.1 mM) and CB[8] (0.15 mM), the aggregation process triggered by the cascade of H_2O_2 (0.3 mM) and pre-proline (0.3 mM) starts at a similar time as when using proline and hydrazide signals. Scattering counts reach 7 Mcps after 50 h, which is slightly higher than observed for proline-triggered aggregation (Figure 2E). This difference may be caused by additional species created in the signal-relay process.

In conclusion, we developed an artificial supramolecular aggregation process capable of responding to chemical signals. We demonstrate a switch between CB [8] binary and ternary host-guest complexes by adjusting the positive charges on bipyridine through a nucleophilic signal-induced reaction with an allylic Michael acceptor. This switch is responsive to a range of biologically relevant nucleophiles such as thiols and amines. We expanded this concept to weak nucleophiles by developing a signal transduction strategy, enabling response to weakly nucleophilic hydrogen peroxide. Using a tripodal bipyridine derivative, we could demonstrate signal-induced supramolecular aggregate formation of CB[8]-cross-linked networks. In this process, the rate of aggregation as well as aggregate structure can be controlled with nucleophile strength. This work offers new opportunities for building more complicated signaling networks and can be expected to pave the way for construction of artificial materials that can interact with living systems through signal transduction and can realize controlled release by reacting to biomarkers.

EXPERIMENTAL PROCEDURES

Resource availability

Lead contact
Further information and requests for resources and reagents should be directed to the lead contact, Rienk Eelkema (R.Eelkema@tudelft.nl).

Materials availability
All experiment data are available upon reasonable request to the lead contact.

Data and code availability
All other data and code supporting the findings of this study are available within the article and are described in the supplemental information or are available from the corresponding author upon reasonable request.

SUPPLEMENTAL INFORMATION

Supplemental information can be found online at https://doi.org/10.1016/j.xcrp.2023.101309.

AUTHOR CONTRIBUTIONS

G.L., R.W.L., and R.E. designed the experiments; Y.W. synthesized the materials; G.L., Y.W., and B.W. conducted the experiments. G.L. and R.E. wrote the manuscript, and all authors commented on the work and the manuscript.

DECLARATION OF INTERESTS

The authors declare no competing interests.

INCLUSION AND DIVERSITY

We support inclusive, diverse, and equitable conduct of research.

REFERENCES

1. Levin, J. (2019). The evolution of mammalian platelets. In Platelets, Third Ed., A.D. Michelson, ed. (Elsevier), pp. 1–23.

2. Gomperts, B.D., Kramer, I.M., and Tatham, P.E.R. (2002). In Signal Transduction B., D. Gomperts, I.M. Kramer, and P.E.R. Tatham, eds. (Elsevier).

3. Yan, X., Wang, F., Zheng, B., and Huang, F. (2012). Stimuli-responsive supramolecular polymeric materials. Chem. Soc. Rev. 41, 6042–6065.

4. Ma, X., and Tian, H. (2014). Stimuli-responsive supramolecular polymers in aqueous solution. Acc. Chem. Res. 47, 1971–1981.

5. Koevoets, R.A., Versteegen, R.M., Kooijman, H., Spek, A.L., Sijbesma, R.P., and Meijer, E.W. (2005). Molecular recognition in a thermoplastic elastomer. J. Am. Chem. Soc. 127, 2999–3003.

6. Appel, E.A., Biedermann, F., Rauwald, U., Jones, S.T., Zayed, J.M., and Scherman, O.A. (2010). Supramolecular cross-linked networks via host-guest complexation with cucurbit[8] uril. J. Am. Chem. Soc. 132, 14251–14260.

7. Jones, C.D., and Steed, J.W. (2016). Gels with sense: supramolecular materials that respond to heat, light and sound. Chem. Soc. Rev. 45, 6546–6596.

8. Del Barrio, J., Horton, P.N., Lairez, D., Lloyd, G.O., Toprakcioglu, C., and Scherman, O.A. (2013). Photocontrol over cucurbit[8]uril complexes: stoichiometry and supramolecular polymers. J. Am. Chem. Soc. 135, 11760–11763.

9. Zou, L., Addonizio, C.J., Su, B., Sis, M.J., Braegelman, A.S., Liu, D., and Webber, M.J. (2021). Supramolecular hydrogels via light-responsive homoternary cross-links. Biomacromolecules 22, 171–182.

10. Yin, Z., Song, G., Jiao, Y., Zheng, P., Xu, J.-F., and Zhang, X. (2019). Dissipative supramolecular polymerization powered by light. CCS Chem. 1, 335–342.

11. Leung, K.C.-F., Chak, C.-P., Lo, C.-M., Wong, W.-Y., Xuan, S., and Cheng, C.H.K. (2009). pH-controllable supramolecular systems. Chem. Asian J. 4, 364–381.

12. Yang, H., Chen, H., and Tan, Y. (2013). Cucurbit [8]uril inducing supramolecular hydrogels by adjusting pH. RSC Adv. 3, 3031–3037.

13. Lin, Y., Li, L., and Li, G. (2013). A new supramolecular gel via host-guest complexation with cucurbit[8]uril and N-(4-diethylaminobenzyl)chitosan. Carbohydr. Polym. 92, 429–434.

14. Liu, Y., Yu, Y., Gao, J., Wang, Z., and Zhang, X. (2010). Water-soluble supramolecular polymerization driven by multiple host-stabilized charge-transfer interactions. Angew. Chem., Int. Ed. 49, 6576–6579.

15. Fukino, T., Yamagishi, H., and Aida, T. (2017). Redox-responsive molecular systems and materials. Adv. Mater. 29, 1603888.

16. Pazos, E., Novo, P., Peinador, C., Kaifer, A.E., and García, M.D. (2019). Cucurbit[8]uril (CB[8])-Based supramolecular switches. Angew. Chem., Int. Ed. 58, 403–416.

17. Xu, W., Song, Q., Xu, J.F., Serpe, M.J., and Zhang, X. (2017). Supramolecular hydrogels fabricated from supramonomers: a novel wound dressing material. ACS Appl. Mater. Interfaces 9, 11368–11372.

18. Shigemitsu, H., and Hamachi, I. (2015). Supramolecular assemblies responsive to biomolecules toward biological applications. Chem. Asian J. 10, 2026–2038.

19. Loh, X.J. (2014). Supramolecular host-guest polymeric materials for biomedical applications. Mater. Horiz. 1, 185–195.

20. Braegelman, A.S., and Webber, M.J. (2019). Integrating stimuli–responsive properties in host–guest supramolecular drug delivery systems. Theranostics 9, 3017–3040.

21. Correia, H.D., Chowdhury, S., Ramos, A.P., Guy, L., Demets, G.J., and Bucher, C. (2019). Dynamic supramolecular polymers built from cucurbit[n]urils and viologens. Polym. Int. 68, 572–588.

22. Zhan, T.G., Zhou, T.Y., Lin, F., Zhang, L., Zhou, C., Qi, Q.Y., Li, Z.T., and Zhao, X. (2016). Supramolecular radical polymers self-assembled from the stacking of radical cations of rod-like viologen di- and trimers. Org. Chem. Front. 3, 1635–1645.

23. Striepe, L., and Baumgartner, T. (2017). Viologens and their application as functional materials. Chem. Eur. J. 23, 16924–16940.

24. Jeon, W.S., Kim, H.J., Lee, C., and Kim, K. (2002). Control of the stoichiometry in host-guest complexation by redox chemistry of guests: inclusion of methylviologen in cucurbit [8]uril. Chem. Commun. 1828–1829.

25. Zhang, Q., Qu, D.-H., Wang, Q.-C., and Tian, H. (2015). Dual-mode controlled self-assembly of TiO 2 nanoparticles through a cucurbit[8] uril-enhanced radical cation dimerization interaction. Angew. Chem., Int. Ed. 54, 15789–15793.

26. Jeon, W.S., Kim, E., Ko, Y.H., Hwang, I., Lee, J.W., Kim, S.-Y., Kim, H.-J., and Kim, K. (2005). Molecular loop lock: a redox-driven molecular machine based on a host-stabilized charge-transfer complex. Angew. Chem. Int. Ed. 44, 87–91.

27. Zhang, L., Zhou, T.Y., Tian, J., Wang, H., Zhang, D.W., Zhao, X., Liu, Y., and Li, Z.T. (2014). A two-dimensional single-layer supramolecular organic framework that is driven by viologen radical cation dimerization and further promoted by cucurbit[8]uril. Polym. Chem. 5, 4715–4721.

28. Jeon, W.S., Ziganshina, A.Y., Lee, J.W., Ko, Y.H., Kang, J.K., Lee, C., and Kim, K. (2003). A [2]pseudorotaxane-based molecular machine: reversible formation of a molecular loop driven by electrochemical and photochemical stimuli. Angew. Chem., Int. Ed. 42, 4097–4100.

29. Sun, S., Zhang, R., Andersson, S., Pan, J., Zou, D., Åkermark, B., and Sun, L. (2007). Host—Guest chemistry and light driven molecular lock of Ru(bpy)3—Viologen with cucurbit[7—8]urils. J. Phys. Chem. B 111, 13357–13363.

30. Vincil, G.A., and Urbach, A.R. (2008). Effects of the number and placement of positive charges on viologen-cucurbit[n]uril interactions. Supramol. Chem. 20, 681–687.

31. Zhang, Z.J., Zhang, Y.M., and Liu, Y. (2011). Controlled molecular self-assembly behaviors between cucurbituril and bispyridinium derivatives. J. Org. Chem. 76, 4682–4685.

32. Zhuang, J., Zhao, B., Meng, X., Schiffman, J.D., Perry, S.L., Vachet, R.W., and Thayumanavan, S. (2020). A programmable chemical switch based on triggerable Michael acceptors. Chem. Sci. 11, 2103–2111.

33. Klemm, B., Lewis, R.W., Piergentili, I., and Eelkema, R. (2022). Temporally programmed polymer – solvent interactions using a chemical reaction network. Nat. Commun. 13, 6242.

34. Lewis, R.W., Klemm, B., Macchione, M., and Eelkema, R. (2022). Fuel-driven macromolecular coacervation in complex coacervate core micelles. Chem. Sci. *13*, 4533–4544.

35. Barrow, S.J., Kasera, S., Rowland, M.J., Del Barrio, J., and Scherman, O.A. (2015). Cucurbituril-based molecular recognition. Chem. Rev. *115*, 12320–12406.

36. National Center for Biotechnology Information. PubChem Compound Summary for CID 23662354. Mesna. https://pubchem. ncbi.nlm.nih.gov/compound/Mesna.

37. Le Goff, G., and Ouazzani, J. (2014). Natural hydrazine-containing compounds: biosynthesis, isolation, biological activities and synthesis. Bioorg. Med. Chem. *22*, 6529–6544.

38. Li, G., Trausel, F., van der Helm, M.P., Klemm, B., Brevé, T.G., van Rossum, S.A.P., Hartono, M., Gerlings, H.H.P.J., Lovrak, M., van Esch, J.H., and Eelkema, R. (2021). Tuneable control of organocatalytic activity through host–guest chemistry. Angew. Chem., Int. Ed. *60*, 14022–14029.

39. Brotzel, F., and Mayr, H. (2007). Nucleophilicities of amino acids and peptides. Org. Biomol. Chem. *5*, 3814–3820.

40. Zhang, K.D., Tian, J., Hanifi, D., Zhang, Y., Sue, A.C.H., Zhou, T.Y., Zhang, L., Zhao, X., Liu, Y., and Li, Z.T. (2013). Toward a single-layer two-dimensional honeycomb supramolecular organic framework in water. J. Am. Chem. Soc. *135*, 17913–17918.

41. Zhang, Q., Xing, R.J., Wang, W.Z., Deng, Y.X., Qu, D.H., and Tian, H. (2019). Dynamic adaptive two-dimensional supramolecular assemblies for on-demand filtration. iScience *19*, 14–24.

42. Wang, Q., Zhang, Q., Zhang, Q.-W., Li, X., Zhao, C.-X., Xu, T.-Y., Qu, D.-H., and Tian, H. (2020). Color-tunable single-fluorophore supramolecular system with assembly-encoded emission. Nat. Commun. *11*, 158.

43. Tian, J., Zhou, T.-Y., Zhang, S.-C., Aloni, S., Altoe, M.V., Xie, S.-H., Wang, H., Zhang, D.-W., Zhao, X., Liu, Y., and Li, Z.T. (2014). Three-dimensional periodic supramolecular organic framework ion sponge in water and microcrystals. Nat. Commun. *5*, 5574.

44. Li, Y., Qin, C., Li, Q., Wang, P., Miao, X., Jin, H., Ao, W., and Cao, L. (2020). Supramolecular organic Frameworks with controllable shape and aggregation-induced emission for tunable luminescent materials through aqueous host–guest complexation. Adv. Opt. Mater. *8*, 1902154.

45. Wang, H., Zhang, D., Zhao, X., and Li, Z.-T. (2019). Chapter 8. Cucurbit[8]uril-based 2D and 3D regular porous Frameworks, pp. 175–192.

46. Boekhoven, J., Poolman, J.M., Maity, C., Li, F., Van Der Mee, L., Minkenberg, C.B., Mendes, E., Van Esch, J.H., and Eelkema, R. (2013). Catalytic control over supramolecular gel formation. Nat. Chem. *5*, 433–437.

47. Liu, X.Y., and Sawant, P.D. (2002). Mechanism of the formation of self-organized microstructures in soft functional materials. Adv. Mater. *14*, 421–426.

48. Liu, X.Y., and Sawant, P.D. (2001). Formation kinetics of fractal nanofiber networks in organogels. Appl. Phys. Lett. *79*, 3518–3520.

49. Barrio, J.D., Liu, J., Brady, R.A., Tan, C.S.Y., Chiodini, S., Ricci, M., Fernández-Leiro, R., Tsai, C.J., Vasileiadi, P., Di Michele, L., et al. (2019). Emerging two-dimensional crystallization of cucurbit[8]uril complexes: from supramolecular polymers to nanofibers. J. Am. Chem. Soc. *141*, 14021–14025.

50. Li, Y., Li, Q., Miao, X., Qin, C., Chu, D., and Cao, L. (2021). Adaptive chirality of an achiral cucurbit[8]uril-based supramolecular organic framework for chirality induction in water. Angew. Chem., Int. Ed. *60*, 6744–6751.

51. Liu, S., Ruspic, C., Mukhopadhyay, P., Chakrabarti, S., Zavalij, P.Y., and Isaacs, L. (2005). The cucurbit[n]uril family: prime components for self-sorting systems. J. Am. Chem. Soc. *127*, 15959–15967.

52. Winterbourn, C.C. (2013). The biological chemistry of hydrogen peroxide. Methods Enzymol. *528*, 3–25.

53. Veal, E.A., Day, A.M., and Morgan, B.A. (2007). Hydrogen peroxide sensing and signaling. Mol. Cell *26*, 1–14.

54. Pravda, J. (2020). Hydrogen peroxide and disease: towards a unified system of pathogenesis and therapeutics. Mol. Med. *26*, 41.

55. Trausel, F., Maity, C., Poolman, J.M., Kouwenberg, D.S.J., Versluis, F., van Esch, J.H., and Eelkema, R. (2017). Chemical signal activation of an organocatalyst enables control over soft material formation. Nat. Commun. *8*, 879.

56. Maity, C., Trausel, F., and Eelkema, R. (2018). Selective activation of organocatalysts by specific signals. Chem. Sci. *9*, 5999–6005.